Supporting Information for

A Bicontinuous Donor-Acceptor Hybrid Heterostructure Based on Coordination and Cation-π Interactions

Meng-Hua Li [a], Ming-Hua You,[a,b] Jiang-Yan Zhang, [a] Wang-Chuan Xiao[c] and Mei-Jin Lin [a*]

[a] *State Key Laboratory of Photocatalysis on Energy and Environment, College of Chemistry, Fuzhou University, China, 350116. E-mail: meijin_lin@fzu.edu.cn.*

[b] *College of Zhicheng, Fuzhou University, China, 350002.*

[c] *School of Resources and Chemical Engineering, Sanming Institute of Fluorochemical Industry, Sanming University, China, 365004*

Table of Contents:

1. Single-crystal X-ray diffraction analysis

Table S1. Crystal Data and Structure Refinements for 1

Complex	**1**
Empirical formula	$C_{23}H_{12}Cu_2N_9S_3$
Formula weight	637.68
Crystal system	triclinic
Space group	P-1
a/Å	9.5199(7)
b/Å	10.2672(6)
c/Å	12.5352(8)
α/°	84.614(5)
β/°	70.854(6)
γ/°	80.244(5)
Volume/Å^3	1139.75(13)
Z	2
Temperature/K	293(2)
ρcalcg/cm^3	1.858
M(Mo Kα)/mm^{-1}	2.177
F(000)	638.0
Reflections collected	15203
Independent reflections	4486 [Rint = 0.0305, Rsigma = 0.0307]
Data/restraints/parameters	4486/2/334
GOF on F^2	1.055
Final R indexes [I>=2σ (I)]	0.0497, 0.1563
Final R indexes [all data]	0.0564, 0.1664
Largest diff. peak/hole / e Å^{-3}	1.44/-2.72

2. Infrared spectral analysis

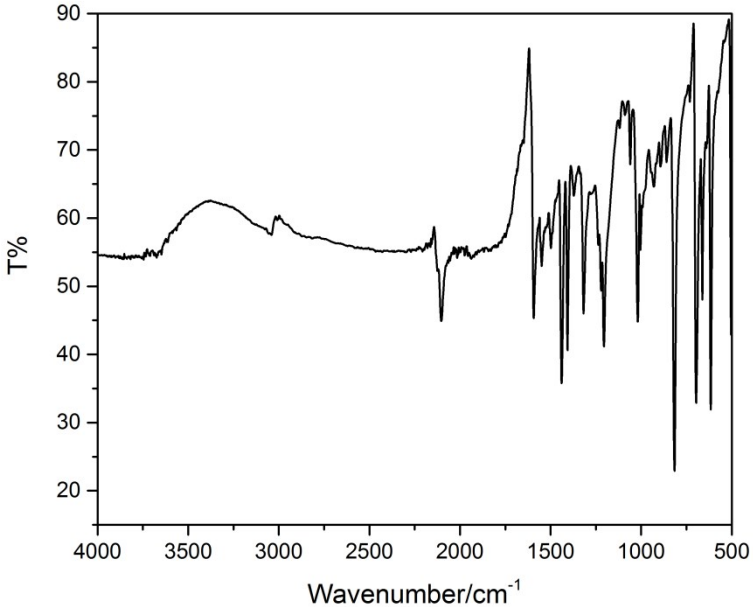

Figure S1. Infrared spectrum of **1**

3. Thermo-gravimetric analysis (TG)

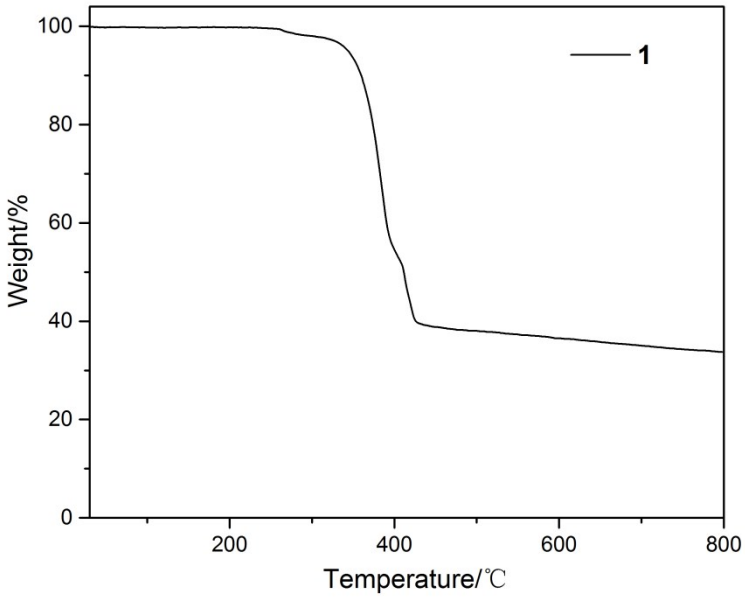

Figure S2. The TG curve of **1** under Ar atmosphere with a heating rate of 10 °C/min.

4. X-ray powder diffraction analysis

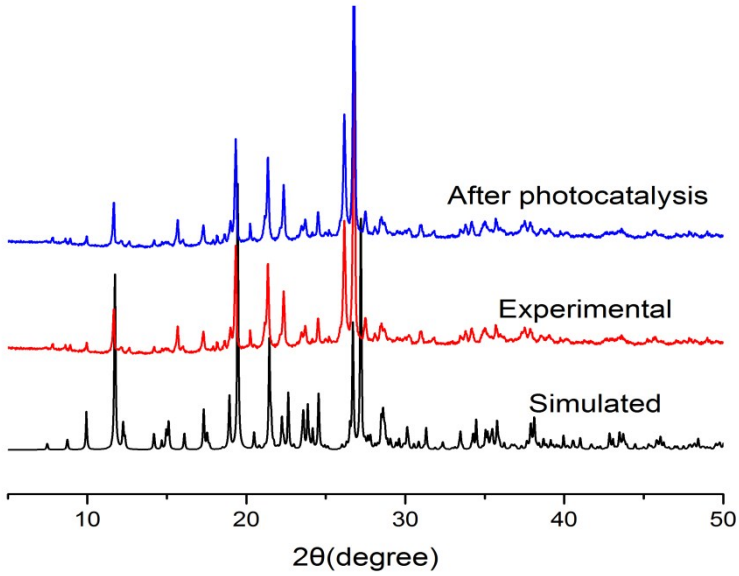

Figure S3. PXRD patterns of **1** before and after the photocatalysis

5. Photocatalytic activity measurements

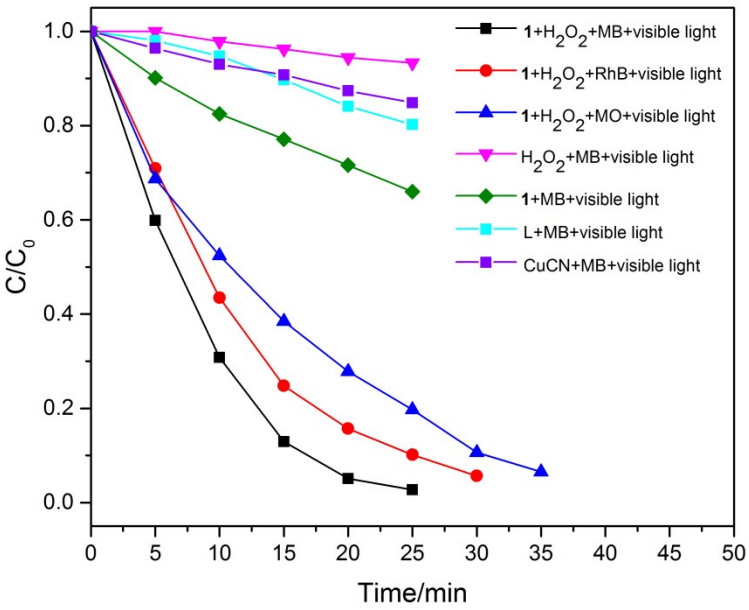

Figure S4. Concentration changes of dyes upon irradiation by visible light as a function of irradiation time with or without the presence of hybrid **1** and H_2O_2, C and C_0 represent the dye concentrations after and before irradiation.

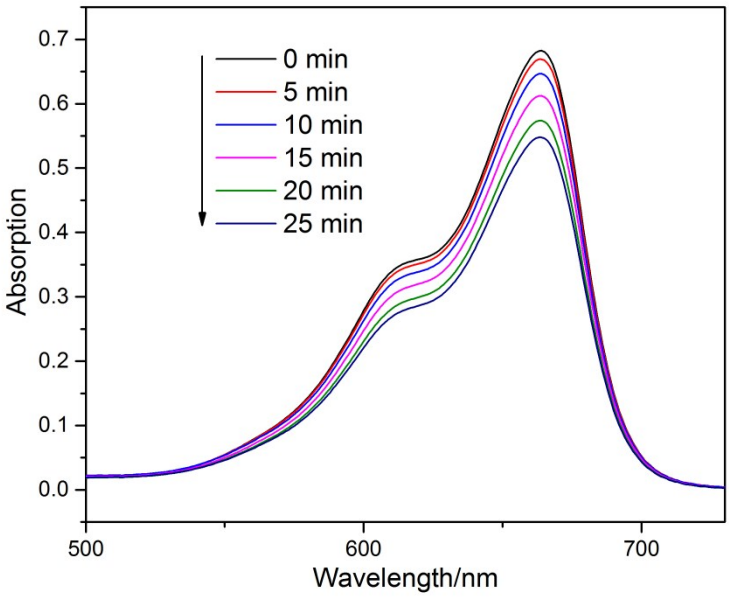

Figure S5. The absorption spectra of the MB solution presence of CuCN under exposure to visible light.

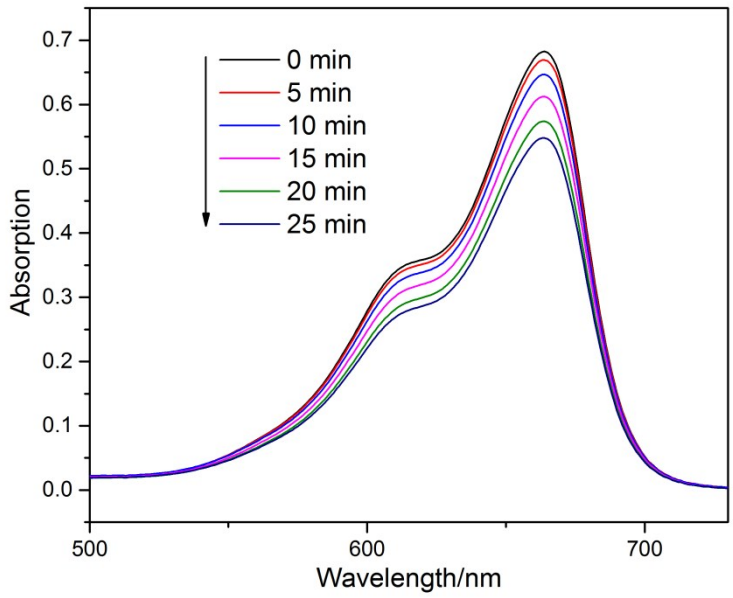

Figure S6. The absorption spectra of the MB solution presence of Py_2TTz under exposure to visible light.

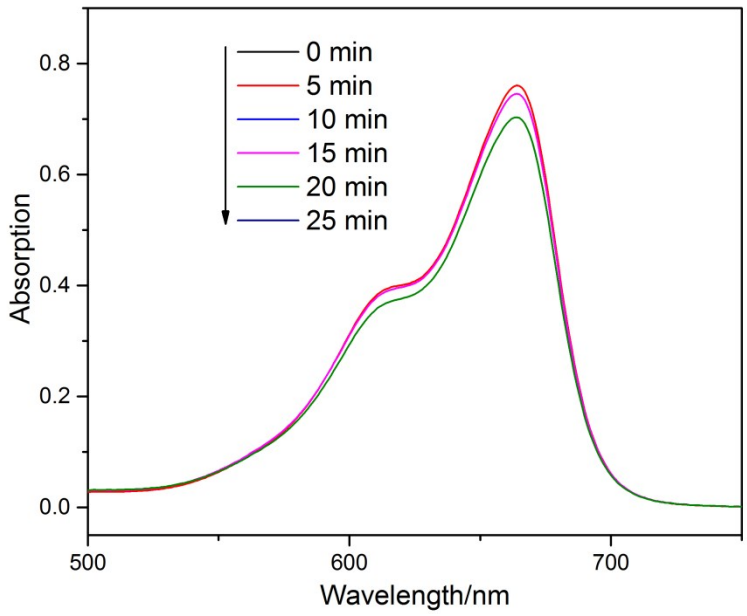

Figure S7. The absorption spectra of the MB solution presence of H_2O_2 under exposure to visible light.

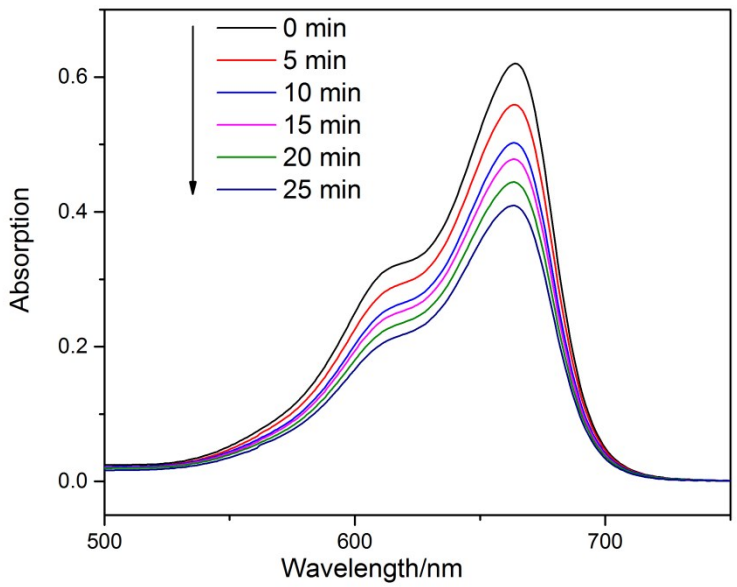

Figure S8. The absorption spectra of the MB solution presence of **1** under exposure to visible light.

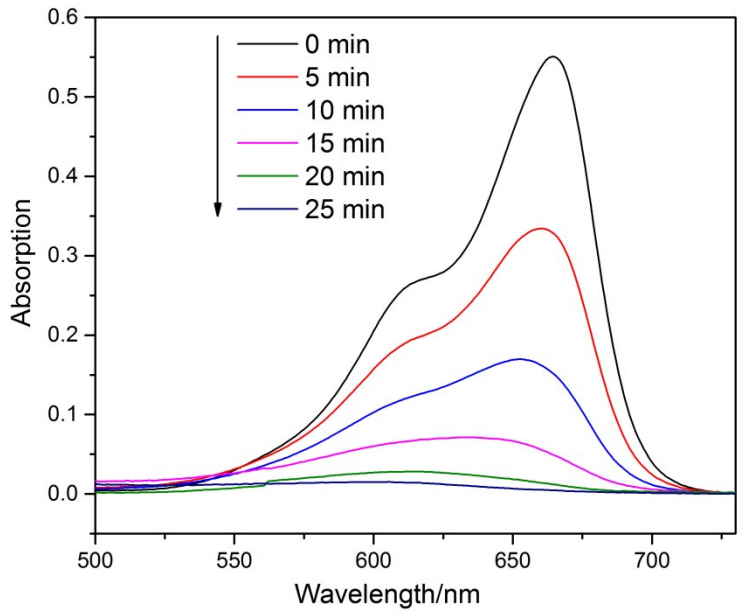

Figure S9. The absorption spectra of the RhB solution presence of **1** together with H_2O_2(400μL, 4.2%) under exposure to visible light.

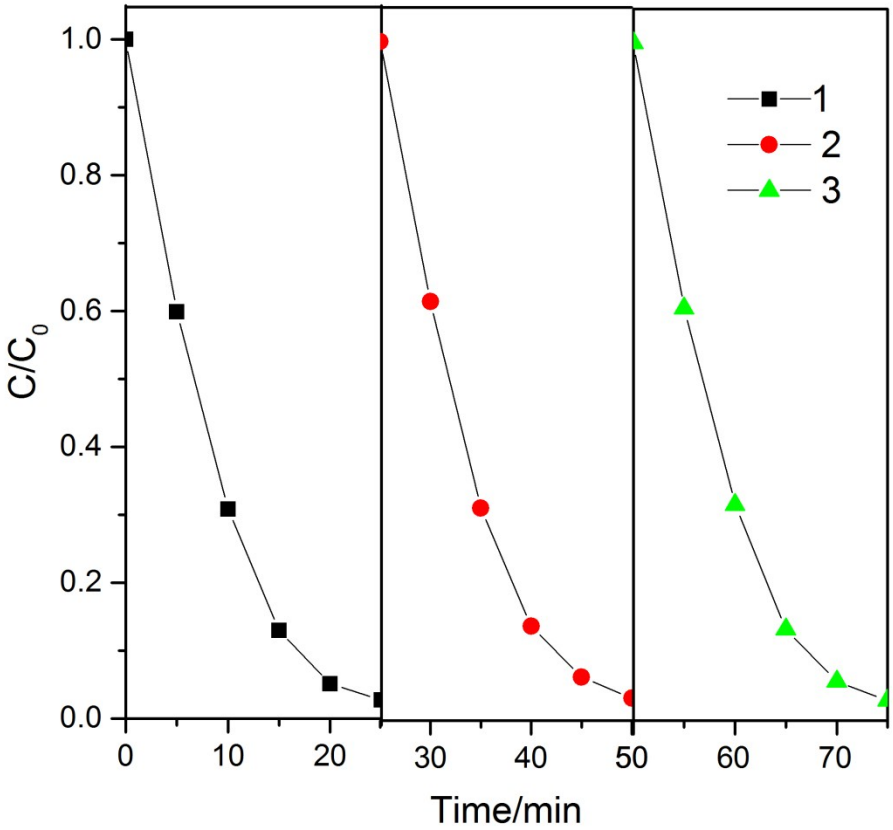

Figure S10. The irradiation-time dependences of the relative concentration C/C_0 of the MB over **1** together with H_2O_2(400μL, 4.2%) during cycling photocatalytic experiments under visible light.

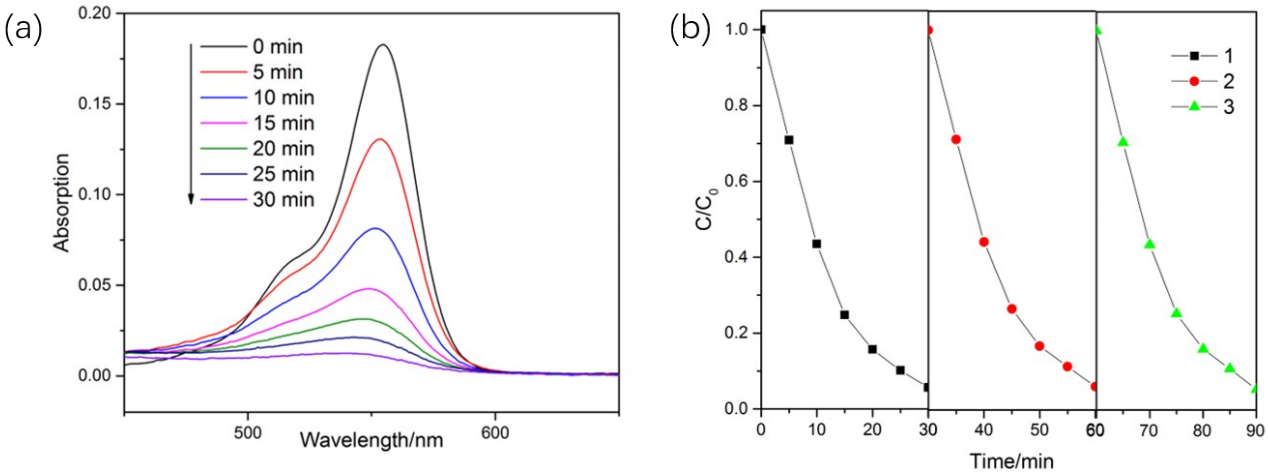

Figure S11. (a) The absorption spectra of the RhB solution in the presence of **1** together with H_2O_2(400 μ L, 4.2%) under exposure to visible light. (b) The irradiation-time dependences of the relative concentration C/C_0 of the RhB over **1** together with H_2O_2(400 μ L, 4.2%) during cycling photocatalytic experiments under visible light.

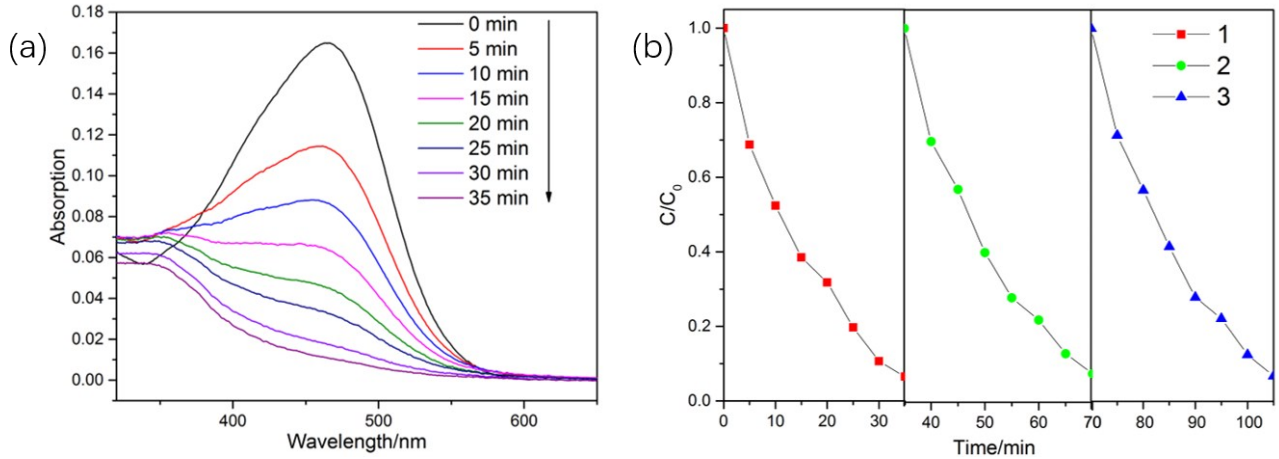

Figure S12. (a) The absorption spectra of the MO solution in the presence of **1** together with H_2O_2(400 μ L, 4.2%) under exposure to visible light. (b) The irradiation-time dependences of the relative concentration C/C_0 of the MO over **1** together with H_2O_2(400 μ L, 4.2%) during cycling photocatalytic experiments under visible light.